Positional Isomerization of Dialkylnaphthalenes: A Comprehensive Interpretation of the Selective Formation of 2,6-DIPN over HM Zeolite

Gyula Tasi,*,†,‡ Fujio Mizukami,† István Pálinkó,§ Makoto Toba,† and Ákos Kukovecz†,‡

Department of Surface Chemistry, National Institute of Materials and Chemical Research, 1-1, Higashi, Tsukuba, Ibaraki 305-8565, Japan, Department of Applied and Environmental Chemistry, University of Szeged, H-6720 Szeged, Rerrich B. tér 1, Hungary, and Department of Organic Chemistry, University of Szeged, H-6720 Szeged, Dóm tér 8, Hungary

Received: September 21, 2000; In Final Form: December 13, 2000

A new ab initio method was developed to supply reliable molecular dimensions for catalytic studies. For the DIPN isomers, calculations at correlated level revealed that the 2,6-isomer has the best molecular shape and dimensions concerning molecular transportation in the channel system of mordenite (M) zeolite. Adsorption rate measurements supported this theoretical finding. According to the ab initio calculations performed at correlated level, the 2,6- and 2,7-DIPN molecules may transform into each other via 1,2-isopropyl shift at an appropriate temperature in the main channel of mordenite. Isomerization reactions of 2,6-DIPN carried out over HM at high temperatures resulted in 2,7-DIPN in the reaction mixture supporting the theoretical results. Theoretical and experimental studies revealed that the selective formation of 2,6-DIPN over HM zeolite is the result of diffusion-controlled shape-selective catalysis, i.e., product selectivity is operative in this case.

Introduction

Acid-catalyzed alkylation of naphthalene with various alkylating agents (alkenes, alcohols, etc.) is of great importance from industrial point of view.[1] Of dialkylnaphthalenes, the 2,6 isomers are starting materials for preparing liquid crystal polymers.[2] Accordingly, many efforts for their selective synthesis are demonstrated in the literature.[3−11] For the selective preparation of 2,6-diisopropylnaphthalene (DIPN) and 2,6-di(*tert*-butyl)-naphthalene (DTBN), HM and HY zeolites,[3,5,6,11] respectively, were found to be the best catalysts. Dealumination to some extent, i.e., decrease in acidity, was observed to further increase their catalytic activities.[6,7] Up to this point, for the rationalization of the experimental results molecular mechanics[11] and semiempirical quantum chemical calculations[9,10] were applied. The selective formation of the 2,6-isomer was explained by either product selectivity[11,12] or spatial transition state selectivity[3,13] or restricted electronic transition state selectivity.[9,10]

Recently, we performed a detailed study concerning the positional isomerization of monoalkylnaphthalenes at various theoretical levels.[14] Ab initio quantum chemical calculations at correlated level revealed that intramolecular migrations are allowed for the methyl, ethyl and isopropyl groups. Moreover, the process becomes easier as the size of the alkyl group increases. In contrast, the bulky *tert*-butyl group transfers exclusively intermolecularly. For the methyl group, we have also studied the possibility of an intermolecular transfer. Calculations with three-body basis set superposition error correction at correlated level revealed that this transfer requires very high activation energy and, thus, it is of low probability compared to the intramolecular one.

In this contribution we prove theoretically as well as experimentally that in contrast with the dimethylnaphthalene (DMN) isomers,[15] the DIPN isomers do not form equilibrium groups. Ab initio calculations at correlated level reveal that the $\beta \rightarrow \beta'$ intramolecular migrations become energetically more and more favorable with the increasing size of the migrating alkyl group: methyl → ethyl → isopropyl. At an appropriate temperature the 2,6- and the 2,7-DIPN molecules may freely transform to one another via intramolecular $\beta \rightarrow \beta'$ isopropyl group migration in the main channel of HM zeolite. Formation of the corresponding transition state complex is not restricted spatially. Results of adsorption rate measurements of the mixture of the DIPN isomers and the calculated ab initio molecular dimensions prove that among the DIPN isomers the 2,6 one moves the easiest, i.e., diffuses the fastest in the main channel of mordenite.

Experimental Section

For the adsorption measurements, 0.5 g of a mixture of some DIPN isomers (Kureha Chemical Co., KMC-113) and 0.2 g of *n*-octadecane (internal standard) were dissolved in 10.0 g of *n*-undecane solvent. 2.0 g of commercial NaM zeolite (Tosoh Chemicals, HSZ-640NAA) outgassed at 473 K for 2 h in high vacuo was then added to the solution, which was kept at 353 K in a silicone oil bath and stirred continuously. Samples for analysis were taken every 5 min and treated as described below. The result of a typical adsorption experiment can be seen in Figure 1.

For the isomerization reaction of 2,6-DIPN over HM, 5.0 g of 2,6-DIPN and 1.0 g of *n*-octadecane (internal standard) were dissolved in 50.0 g of *n*-undecane. After the analysis of the initial mixture, the solution was transferred into a 100 cm^3 stainless steel autoclave and mixed with 5.0 g of commercial HM zeolite (Tosoh Chemicals, HSZ-660HOA) outgassed at 573 K for 2 h in high vacuo. The reaction mixture was stirred (700 rpm) at 513 K for 5 h, then the reaction was stopped and a sample was withdrawn for analysis. Results of a typical isomerization experiment are shown in Table 1.

† Department of Surface Chemistry.
‡ Department of Applied and Environmental Chemistry.
§ Department of Organic Chemistry.

10.1021/jp003428t CCC: $20.00
Published on Web 06/09/2001

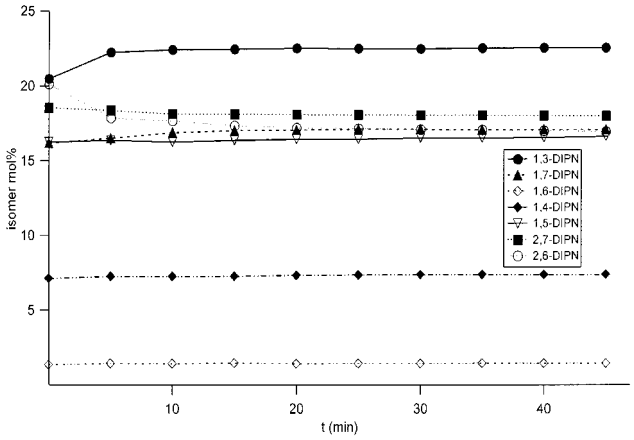

Figure 1. Adsorption of the mixture of DIPN isomers on NaM at 353 K.

TABLE 1: Isomerization of 2,6-DIPN over HM Zeolite at 513 K

DIPN isomer	mol % ($t = 0$)	mol % ($t = 5$ h)
1,3	0	0.35
1,7	0	0.23
1,6	0	0.17
2,7	0	3.32
2,6	100	95.93

For quantitative analysis, 0.1 cm^3 slurry was taken via a syringe. This amount was diluted with *n*-undecane to 1.0 cm^3, centrifuged at 5000 rpm for 1 min and, finally, 0.5 cm^3 of the resulting clear solution was loaded into the autosampler of a Shimadzu GC17A gas chromatograph equipped with a flame ionization detector and a 60 m × 0.25 mm × 0.25 m OV-1 capillary column. Using a temperature program (10 K/min from 373 to 443 K with a 8 min hold at 443 K, then 5 K/min from 443 to 523 K with a 19 min hold at 523 K), retention times were as follows: 29.56 min for 1,3-DIPN, 29.73 min for 1,7-DIPN, 30.16 min for 1,6-DIPN, 30.6 min for 1,4-DIPN, 30.81 min for 1,5-DIPN, 31.05 min for 2,7-DIPN, 31.3 min for 2,6-DIPN, and 33.7 min for the *n*-octadecane internal standard.

Computational Methods

For the ab initio and semiempirical quantum chemical calculations, the Gaussian98[16] and PcMol[17] packages were used. For determining the most stable conformers of molecules with conformational flexibility, methods applied for aliphatic alkanes were used.[18] In this work, if otherwise not stated, each molecule is represented by its most stable conformer. For drawing and analyzing molecular structures, the gOpenMol package[19] was applied.

The following notation is used to designate the ab initio quantum chemical computational results: HF, HF/6-31G*//HF/6-31G*; MP2, MP2(full)/6-31G*//MP2(full)/6-31G*; and G2-(MP2,SVP).[20c] Details concerning the methods and the basis sets applied are given in the literature.[21] G2(MP2,SVP) energy calculations on MP2(full)/6-31G* optimized geometries approximate energies at the QCISD(T)/6-311+G(3df,2p) level. Actually, the evaluation of the G2(MP2,SVP) energy requires only two single-point calculations: QCISD(T)/6-31G* and MP2(FC)/6-311+G(3df,2p).

Calculation of zero-point vibrational energy (ZPVE) corrections and thermochemical quantities was performed within the rigid rotor-harmonic oscillator (RRHO) approximation.[22] Scaled HF/6-31G*//HF/6-31G* harmonic vibrational frequencies were used in every case, exactly as in the Gaussian methods.[20] Recently, the RRHO approximation was successfully applied for calculating various thermochemical quantities for aliphatic alkanes.[18,23]

The trial geometries for the transition state calculations were generated with the help of the PcMol package. The characterization of the stationary points obtained was performed by harmonic vibrational analysis at both HF and MP2 levels. For every transition state, the local minima connected by the transition state in question were determined by an intrinsic reaction coordinate calculation.[24]

As far as shape-selective catalysis is concerned, molecular shape and size are properties of utmost importance.[25,26] Therefore, a reliable ab initio method is needed for determining them.

To the best of our knowledge, so far mechanistic models have been used[3,4,9−11] in theoretical studies concerning shape-selective catalysis: possessing a molecular geometry (from molecular mechanical or semiempirical quantum chemical calculations) and atomic van der Waals radii, the molecular surface is obtained as the superposition of rigid atomic spheres (fused-spheres models). The dimensions of the generated molecular shape are then determined by means of molecular graphics. This procedure, however, cannot be taken as a reliable quantitative method.

By quantum mechanics, the molecular shape is determined by the spatial distribution of electrons in the molecule.[27] Consequently, it can be generated from three-dimensional (3D) electron density maps. For instance, the popular Gaussian program packages allow one to calculate the electron density $\rho(x, y,z)$ at high level of theory at the points of a large 3D grid around the molecule. From these data, points on the ab initio molecular surface (isosurface) can be generated via interpolation using a reliable cutoff value (ρ_0 = constant). To visualize our molecular surfaces on a graphical display, triangulations may also be performed using, for instance, the marching cubes algorithm.[28]

For determining the ab initio molecular surface and shape, 3D grids consisting of 400 × 400 × 400 points were taken around each molecule in this work. The electron density was calculated at the MP2 level of theory, i.e., including important dynamic electron correlation effects. For each conformer of the molecules studied, a sequence of molecular shapes and dimensions was generated using a set of cutoff values: {0.0005, 0.001, 0.002, 0.003, 0.004, 0.005}. However, since the differences in shapes and dimensions were consistent on each isodensity level, only the results obtained with $\rho_0 = 0.001$ au are presented in our paper. This "calibration" was based on adsorption measurements and the published effective pore sizes of zeolite structures. However, let us emphasize once again that the relative molecular dimensions of alkyl- and dialkylnaphthalenes do not depend on the particular value of the cutoff parameter. Further benchmark calculations on various small molecules also supported our chosen cutoff value. For instance, the dimensions of the nitrogen and oxygen molecules (in $Å^3$) determined by the method described in the next paragraph were 3.65 × 3.65 × 4.75 and 3.45 × 3.45 × 4.55, respectively. The results are in very good agreement with the published kinetic diameters:[29] nitrogen, 3.64 Å, and oxygen, 3.46 Å. The small difference in their molecular sizes allows one to separate them from air using an appropriate zeolite adsorbent.

Having obtained the ab initio molecular shapes, the molecular dimensions were calculated via parameter estimation.[30] For the dialkylnaphthalene molecules, we have determined the smallest parallelepipeds enclosing their molecular shapes. To a good approximation, the dimensions of the optimum parallelepipeds

can be regarded as the dimensions of the molecules under consideration. Since three parameters determine the spatial orientation of a molecule in the laboratory coordinate system, our parameter space is three-dimensional. The parameters may be the rotational angles around the axes of the laboratory coordinate system.

Obviously, instead of using a parallelepiped other 3D solid objects (sphere, right circular cylinder, etc.) may be considered. However, the main channel of mordenite can be taken as an elliptical cylinder[31] of 6.7 Å × 7.0 Å which may be further distorted in the course of diffusion of guest molecules, thus, the use of a parallelepiped seems to be well justified.

Generally, optimization procedures afford more than one local minimum. The problem can be circumvented by determining all the local minima and selecting the best one, i.e., the global minimum. Since the parameter space is only three-dimensional in our case, this procedure is feasible: it can be performed with relative ease. However, one more criterion has to be taken into account: one of the cross sections of the optimum parallelepiped should be the smallest possible as well.

The procedure described above is fully automatic. Our FORTRAN codes have been linked to the Gaussian98 program package. Further details are given elsewhere.[32]

Calculations were performed on IBM SP supercomputers as well as on IBM RISC/6000 and PC workstations.

Results and Discussion

In a previous paper we have discussed electrophilic aromatic substitution reactions with special attention to the monoalkylation of naphthalene.[14] Therefore, the most important findings are only highlighted in the following paragraph.

Experiments and calculations revealed that while the α-position is the most reactive, the β-position is the most stable site in the naphthalene molecule concerning electrophilic alkylation reactions. Accordingly, the initial (kinetic) regioselectivity favors the formation of the α-isomer, while the thermodynamic regioselectivity prefers that of the β-isomer. Thermodynamic equilibrium will be established if the isomers are able to transform to each other, i.e., the corresponding transition states are easily formed. If the temperature is too low, or the formation of the transition sate is spatially restricted, the initial regioselectivity will predominate. The rate-determining step of the alkylation reactions under consideration is the formation of the σ-complexes (alkylarenium ions) and their further transformations. For instance, the alkylarenium ions may transform to each other via intra- or intermolecular alkyl group migrations. For the methyl, ethyl and isopropyl groups, intramolecular transfers (1,2-alkyl shifts) are possible. Moreover, for monoalkylnaphthalenes the activation energies of the 1,2-alkyl shifts decrease with the size of the migrating alkyl group. As far as the 1,2-methyl shifts are concerned, the $\beta \rightarrow \alpha$ and $\alpha \rightarrow \beta$ shifts are much more favored energetically than the $\beta \rightarrow \beta'$ and $\alpha \rightarrow \gamma$ ones. It is noteworthy that the *tert*-butyl group seems to be too bulky to take part in an intramolecular transfer. For monoalkylnaphthalenes, the calculated equilibrium compositions obtained at the MP2 level are in good agreement with the experimental results. As the size of the alkyl substituent increases, the β-isomer becomes more and more stable than the α-isomer. For methylnaphthalenes, the G2(MP2,SVP) results precisely match the experimental values. Unfortunately, the G2(MP2,SVP) calculations are not feasible for large molecules: they use huge amounts of CPU time and require large hard disk capacities.

According to the relative positions of the two alkyl substituents, the 10 isomers of dialkylnaphthalenes may be classified into the following groups: (α, α′) {1,4; 1,5; 1,8}, (α, β) {1,2; 1,3; 1,6; 1,7}, and (β, β') {2,3; 2,6; 2,7}. For the diisopropyl derivatives, it is worthwhile to determine and compare their molecular sizes.

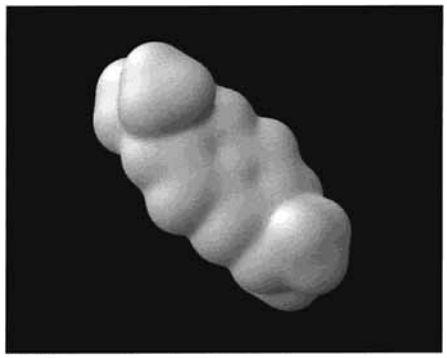

Figure 2. Ab initio (MP2) molecular shape of the most stable conformer of 2,6-DIPN.

TABLE 2: Molecular Dimensions (*a*, *b*, and *c* in angstroms) of the Most Stable Conformers of the DIPN Isomers at the MP2 Level of Theory

group	isomer	*a*	*b*	*c*	rank
(α,α′)	1,4	6.22	9.46	12.05	9
	1,5	6.45	8.78	12.44	4
	1,8	6.59	9.99	10.16	8
(α,β)	1,2	6.95	8.72	11.69	5
	1,3	6.89	9.96	11.84	10
	1,6	6.81	8.10	13.17	3
	1,7	6.87	8.96	11.84	6
(β,β')	2,3	6.76	9.86	11.35	7
	2,6	6.61	6.61	14.23	1
	2,7	6.62	7.26	13.76	2

With the help of mechanistic models,[3,4,9−10] the following conclusions had been made: (i) as far the sizes of the isomers are concerned it is valid that (α,α′) > (α,β) > (β,β'); (ii) the sizes of the 2,6- and the 2,7-DIPN molecules are the same or very close to each other; and (iii) since the 2,6-DIPN isomer is more "linear" than the 2,7 one, it diffuses faster in the main channel of mordenite. Interestingly, the "more linear structure" of the 2,6-DIPN molecule was not revealed in the computed molecular dimensions, i.e., statements ii and iii are contradictory.

Table 2 contains the optimum molecular dimensions obtained by our method. Calculations refer to the ab initio (MP2) shape of the most stable conformers as has been discussed above. For each molecular shape, 7−10 different local minima (optimum parallelepipeds) were obtained. Table 2 contains the best values, i.e., the global minima. It is clearly seen that the dimensions of the 2,6-isomer are the best: its cross section of 6.61 Å × 6.61 Å perfectly fits into the elliptical main channel of mordenite (6.7 Å × 7.0 Å). The second best is the 2,7-isomer with a cross section of 6.62 Å × 7.26 Å.

It is to be seen that the dimensions of the most stable conformers of 2,6- and the 2,7-DIPN differ considerably. Consequently, the mechanistic models in question led to erroneous conclusions. Figures 2 and 3 display the ab initio molecular shapes of the most stable conformers of 2,6- and 2,7-DIPN, respectively. It can be seen that the 2,6-isomer is more "linear" than the 2,7 one, which is, however, revealed in our numerical results as well.

It is also worthwhile to evaluate the molecular dimensions of the less stable conformers of the 2,6- and 2,7-DIPN molecules. The results are summarized in Table 3. It is to be seen that three nonisomorphic conformers were found for both molecules at the HF and MP2 levels of theory, while recent

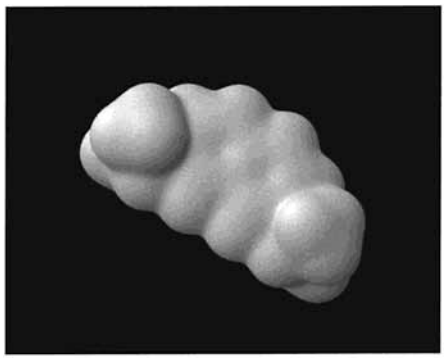

Figure 3. Ab initio (MP2) molecular shape of the most stable conformer of 2,7-DIPN.

TABLE 3: Molecular Dimensions (*a*, *b*, and *c* in angstroms) and Total Energies (au) of the Conformers of 2,6- and 2,7-DIPN at the MP2 Level of Theory[a]

isomer	conformers	total energy	*a*	*b*	*c*
2,6-DIPN	I (C_{2h})	−619.40525	6.61	6.61	14.23
	II (C_s)	−619.40462	6.69	7.09	14.10
	III (C_{2h})	−619.40395	6.44	7.06	14.12
2,7-DIPN	I (C_{2v})	−619.40518	6.62	7.26	13.76
	II (C_s)	−619.40454	6.70	8.05	13.30
	III (C_{2v})	−619.40388	6.73	8.40	12.57

[a] Total energies are at 0 K and include ZPVE corrections.

TABLE 4: Activation Energies (kJ/mol) of Some Intramolecular Alkyl Group Transfers at 0 K with ZPVE Corrections at the MP2 Level of Theory

compound	2,6 → 2,7	2,7 → 2,6	1,5 → 1,6	1,6 → 1,5
DMN	99.34	92.92	65.69	52.02
DETN	85.89	79.40	53.58	38.96
DIPN	64.65	58.84	46.71	33.49

semiempirical calculations[9,10] provided only two. On the basis of data presented in Table 3, one can conclude that the molecular dimensions of the less stable conformers are larger than those of the global minima. For the 2,6-isomer, however, the dimensions move around the magic cross section of 6.7 Å × 7.0 Å. In contrast, dimensions of the less stable conformers of 2,7-DIPN are considerably larger than those of the global minimum. From this it follows that they enter the main channel of mordenite with much more difficulties if they can enter at all.

After all these considerations, the experiment displayed in Figure 1 can be easily rationalized. The 2,6-DIPN molecule can enter the main channel of mordenite and diffuse in there the easiest. In addition, this statement holds true for each conformer of the molecule. It is noteworthy that molecular mechanics calculations[11] also support these findings.

Besides the molecular shape and size, thermodynamic properties of the isomers are of utmost importance: they determine the thermodynamic equilibrium composition of the mixture of the isomers under conditions of free isomerization.

Analysis of the HF−BF_3-catalyzed isomerization of DMN isomers revealed that the isomers belong to four equilibrium sets, and there is no interconversion among them.[15] The existence of isolated equilibrium groups is the result of the very high activation energy of the $\beta \rightarrow \beta'$ 1,2-methyl shifts. These activation energies are far larger than those of the $\alpha \rightarrow \beta$ and the $\beta \rightarrow \alpha$ shifts.

Table 4 shows the calculated activation energies for the interconversion of 2,6- and 2,7-isomers via a 1,2-alkyl shift at the MP2 level of theory. The table also contains the calculated values for the interconversion of the 1,5- and 1,6-isomers. On the basis of these data, the following conclusions may be drawn: (i) on increasing the size of the alkyl group the activation energies decrease considerably and (ii) for the DIPN isomers the activation energies of the $\beta \rightarrow \beta'$ shifts are comparable to those of the $\alpha \rightarrow \beta$ and $\beta \rightarrow \alpha$ shifts of the DMN isomers. Therefore, the calculation results suggest that the 2,6- and 2,7-DIPN molecules are able to transform to each other intramolecularly via 1,2-isopropyl shift at an appropriate temperature. This is a very important theoretical finding from the viewpoint of mordenite, since in its main channel there is not enough room for an intermolecular transfer. In the transition state of an intermolecular transfer the migrating alkyl group is located between two naphthtalene rings, thus, the size of the transition complex is very large (see Figure 7 in ref 14).

As far as the isomerization of 2,6-DIPN is concerned, the 2,7-isomer is formed in the reaction (see data in Table 1) verifying the conclusions derived from the calculation results. However, formation of 1,3-DIPN indicates that dealkylation-realkylation reactions should also be taken into account, although their proportions are not large. Experimental as well as computational results unequivocally show that the DIPN isomers can freely interconvert in HM zeolite, i.e., equilibrium sets are not formed. The computational results in the next paragraph rationalize the experimental observation concerning the occurrence of only certain DIPN isomers in the reaction mixture.

Table 5 displays the calculated and the experimental thermodynamic equilibrium compositions of the mixtures of DMN and DIPN isomers. On calculation it was assumed that the mixture of the isomers is ideal.[33] Details concerning the calculation of the equilibrium fractions of the isomers can be found in our previous paper.[14] For the DMN isomers, calculations were performed either assuming the existence of equilibrium groups or without this hypothesis. This means that in the latter case free interconversion was assumed among the isomers. For the DIPN isomers, conditions of free isomerization were

TABLE 5: Equilibrium Compositions of the Mixtures of DMN and DIPN Isomers at Different Theoretical Levels (298.15 K, 1 atm)[a]

		equilibrium sets								
			II			III			IV	
compound	method	I (1,2)	1,3	1,4	2,3	1,7	1,8	2,7	1,5	1,6	2,6
	HF		65.8	1.0	33.2	7.5	0.0	92.5	0.1	10.1	89.8
DMN	MP2		59.3	4.7	36.0	33.0	0.0	67.0	2.3	30.6	67.2
	G2(MP2,SVP)		66.0	5.9	28.1	37.6	0.0	62.4	4.1	37.9	58.0
	exptl		64	1	35	39	0	61	3	40	57
	MP2[b]	0.3	13.0	1.0	7.9	12.6	0.0	25.5	0.9	12.2	26.7
	G2(MP2,SVP)[b]	0.6	15.3	1.4	6.5	14.0	0.0	23.2	1.6	14.8	22.7
DIPN	HF[b]	0.0	0.1	0.0	0.0	0.1	0.0	51.9	0.0	0.1	47.9
	MP2[b]	0.0	2.1	0.0	0.1	1.7	0.0	46.0	0.0	1.5	48.7

[a] Experimental values are from ref 15. [b] Free interconversion is assumed among the isomers, i.e., equilibrium sets are not formed.

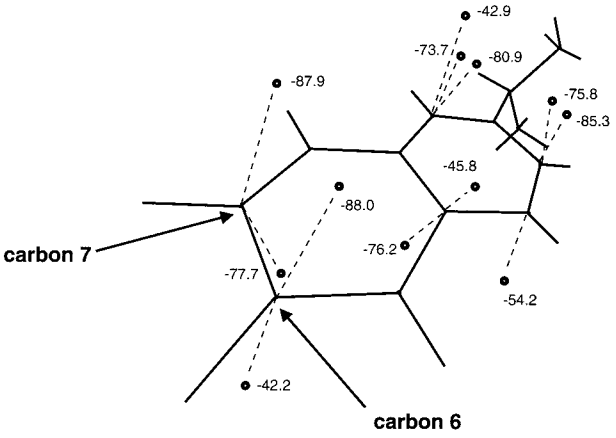

Figure 4. Some MEP local minima for the 2-IPN molecule at the HF level of theory.

applied on the basis of the arguments discussed above. It is to be seen that for the DMN isomers the G2(MP2,SVP) results are in complete accordance with the experimental ones and the MP2 values are also accurate enough. For the DIPN molecules, the 2,6- and 2,7-isomers are far more stable than the others. Computational results predict that, beside the 2,6 and 2,7 DIPN isomers, the 1,3, 1,6, and 1,7 ones should also be found in detectable amounts in the equilibrium mixture. Data of Table 1 unambiguously support this statement.

Recently, the frontier molecular orbital (FMO) method[34] was applied to shed light on the selective formation of 2,6-DIPN over HM zeolite.[9,10] With semiempirical quantum chemical calculations, it was found that the frontier electron density on carbon 6 is greater than that on carbon 7 in the 2-IPN molecule. On the basis of this result, it was claimed that electronic factors favor 2,6-DIPN over 2,7-DIPN. The selectivity in question was named restricted electronic transition state selectivity.[9,10]

However, the electronic factors under consideration should reveal themselves in molecular electrostatic potential (MEP) maps. As a matter of fact, MEP as a rigorously defined quantum mechanical property[35] can be successfully used to rationalize, for instance, the initial selectivity of electrophilic alkylations of aromatics[14,36] and fused N-heteroaromatics.[37] For the 1- and 2-IPN molecules, we have determined all the MEP local minima at the HF and MP2 levels of theory. The calculations resulted in about 50 different local minima in both cases. Some of them are displayed in Figure 4 for 2-IPN. In the figure dashed lines connect the locations of the minima to the nearest atoms. In addition, Figure 5 shows the ChelpG EP atomic charges for the 1- and 2-IPN molecules at the MP2 level of theory. It is clearly seen that molecular electrostatics at ab initio level does not distinguish between positions 6 and 7 in the molecules in question concerning electrophilic aromatic substitution reactions. Therefore, it should be concluded that the semiempirical frontier electron density values are misleading in this case.

Conclusion

The ab initio molecular shape of 2,6-DIPN much better fits into the main channel of mordenite than that of the 2,7-isomer. Moreover, this holds true for all the conformers of the molecules in question. In accordance with the calculation results, adsorption rate measurements revealed that the 2,6-DIPN molecule diffuses the fastest in the channel system of mordenite.

According to the calculation results obtained at correlated level, the 2,6- and 2,7-DIPN molecules may transform to each other via 1,2-isopropyl shift at an appropriate temperature.

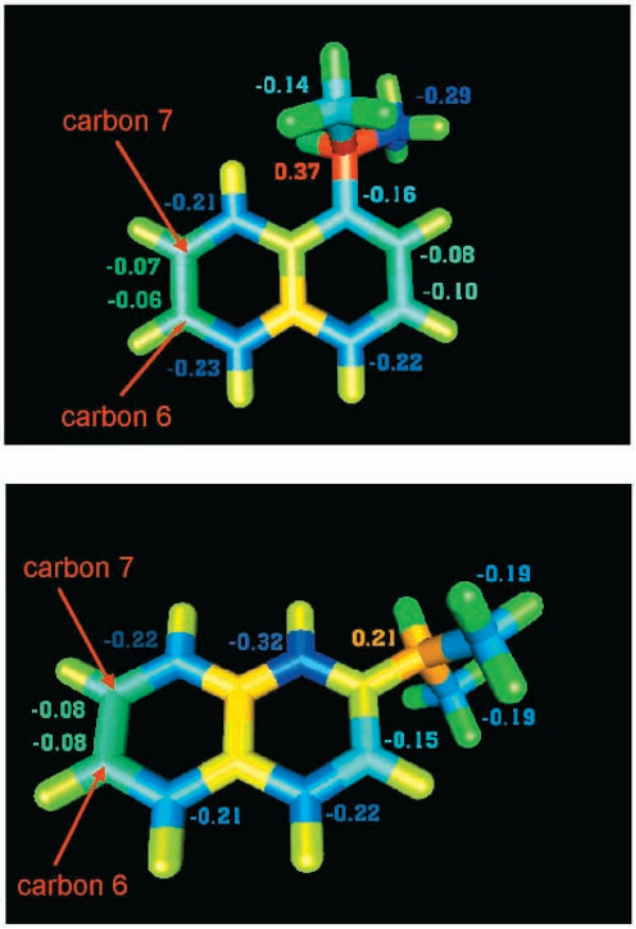

Figure 5. EP atomic charges for the 1-IPN and 2-IPN molecules at the MP2 level of theory.

Furthermore, the 2,6- and 2,7-isomers are the most stable DIPN isomers: under free isomerization conditions they have the largest concentrations in the reaction mixture.

Molecular electrostatics at ab initio level does not distinguish between carbon 6 and carbon 7 in the 1- and 2-IPN molecules indicating that the restricted electronic transition state concept based on semiempirical frontier electron density values is false.

All in all, theoretical and experimental results reveal that the most stable 2,6- and 2,7-isomers of DIPN can intramolecularly transform to each other in the main channel of HM zeolite and the 2,6-isomer can leave the bulk phase of mordenite the fastest. The selective formation of 2,6-DIPN over HM zeolite is the result of diffusion-controlled shape-selective catalysis.

Acknowledgment. The work was sponsored by the Agency of Industrial Science and Technology (AIST) and the New Energy and Industrial Technology Development Organization (NEDO).

References and Notes

(1) Olah, G. A.; Molnár, Á. *Hydrocarbon Chemistry*; John Wiley & Sons: New York, 1995; pp 102−198.
(2) Song, C.; Schobert, H. H. *Fuel. Process. Technol.* **1993**, 157.
(3) Katayama, A.; Toba, M.; Takeuchi, G.; Mizukami, F.; Niwa, S.; Mitamura, S. *J. Chem. Soc., Chem. Commun*. **1991**, 39.
(4) Moreau, P.; Finiels, A.; Geneste, P.; Joffre, J.; Moreau, F.; Solofo, J. *Catal. Today* **1996**, *31*, 11.
(5) Liu, Z.; Moreau, P.; Fajula, F. *J. Chem. Soc., Chem. Commun*. **1996**, 2653.
(6) Liu, Z.; Moreau, P.; Fajula, F. *Appl. Catal., A* **1997**, *159*, 305.
(7) Chu, S.; Chen, Y. *Appl. Catal., A* **1995**, *123*, 51.
(8) Brzozowski, R.; Tecza, W. *Appl. Catal., A* **1998**, *166*, 21.

(9) Song, C.; Ma, X.; Schmitz, A. D.; Schorbert, H. H. *Appl. Catal., A* **1999**, *182*, 175.

(10) Song, C.; Ma, X.; Schorbert, H. H. *ACS Symp. Ser.* **1999**, *738*, 305.

(11) Horsley, J. A.; Fellmann, J. D.; Derouane, E. G.; Freeman, C. M. *J. Catal*. **1994**, *147*, 231.

(12) Kikuchi, E.; Sawada, K.; Maeda, M.; Matsuda, T. *Stud. Surf. Sci. Catal.* **1994**, *90*, 391.

(13) Kim., J.; Sugi, Y.; Matsuzaki, T.; Hanaoka, T.; Kubota, Y.; Tu, X.; Matsumoto, M. *Microporous Mater.* **1995**, *5*, 113.

(14) Tasi, G.; Mizukami, F.; Makoto, T.; Niwa, S.; Pálinkó, I. *J. Phys. Chem. A* **2000**, *104*, 1337.

(15) Suld, G.; Stuart, A. P. *J. Org. Chem.* **1964**, *29*, 2939.

(16) Frisch, M. J.; Trucks, G, W.; Schlegel, H. B.; Scuseria, G. E.; Robb, M. A.; Cheeseman, J. R.; Zakrzewski, V. G.; Montgomery, J. A., Jr.; Stratmann, R. E.; Burant, J. C.; Dapprich, S.; Millam, J. M.; Daniels, A. D.; Kudin, K. N.; Strain, M. C.; Farkas, O.; Tomasi, J.; Barone, V.; Cossi, M.; Cammi, R.; Mennucci, B.; Pomelli, C.; Adamo, C.; Clifford, S.; Ochterski, J.; Petersson, G. A.; Ayala, P. Y.; Cui, Q.; Morokuma, K.; Malick, D. K.; Rabuck, A. D.; Raghavachari, K.; Foresman, J. B.; Cioslowski, J.; Ortiz, J. V.; Stefanov, B. B.; Liu, G.; Liashenko, A.; Piskorz, P.; Komaromi, I.; Gomperts, R.; Martin, L. R.; Fox, D. J.; Keith, T.; Al-Laham, M. A.; Peng, C. Y.; Nanayakkara, A.; Gonzalez, C.; Challacombe, M.; Gill, P. M. W.; Johnson, B.; Chen, W.; Wong, M. W.; Andres, J. L.; Gonzalez, C.; Head-Gordon, M.; Replogle, E. S.; Pople, J. A. *Gaussian 98*, Revision A.6; Gaussian, Inc.: Pittsburgh, PA, 1998.

(17) Tasi, G.; Pálinkó, I.; Halász, J.; Náray-Szabó, G. *Semiempirical Calculations on Microcomputers*; CheMicro Limited: Budapest, 1992.

(18) Tasi, G.; Mizukami, F.; Pálinkó, I.; Csontos, J.; Gyorffy, W.; Nair, P.; Maeda, K.; Toba, M.; Niwa, S.; Kiyozumi, Y.; Kiricsi, I. J. *Phys. Chem. A* **1998**, *102*, 7698. Tasi, G.; Mizukami, F. *J. Chem. Inf. Comput. Sci.* **1998**, *38*, 632. Tasi, G.; Mizukami, F. *J. Math. Chem.* **1999**, *25*, 55.

(19) Laaksonen, L. *gOpenMol*, version 1.30 (a program for drawing and analyzing molecular structures); 1999.

(20) (a) Pople, J. A.; Head-Gordon, M.; Fox, D. J.; Raghavachari, K.; Curtiss, L. A. *J. Chem. Phys.* **1989**, *90*, 5622. (b) Curtiss, L. A.; Raghavachari, K.; Trucks, G. W.; Pople, J. A. *J. Chem. Phys.* **1991**, *94*, 7221. (c) Curtiss, L. A.; Redfern, P. C.; Smith, B. J.; Radom, L. *J. Chem. Phys.* **1996**, *104*, 5148. (d) Curtiss, L. A.; Raghavachari, K.; Redfern, P. C.; Rassolov, V.; Pople, J. A. *J. Chem. Phys.* **1998**, *109*, 7764.

(21) (a) Hehre, W. J.; Radom, L.; Schleyer, P. v. R.; Pople, J. A. *Ab initio Molecular Orbital Theory*; John Wiley & Sons: New York, 1986. (b) Szabo, A.; Ostlund, N. S. *Modern Quantum Chemistry*; Dover Publications: New York, 1996. (c) Cook, D. B. *Handbook of Computational Quantum Chemistry*; Oxford University Press: Oxford, 1998.

(22) McQuarrie, D. A. *Statistical Mechanics*; Harper & Row: New York, 1976; pp 129−139.

(23) DeTar, D. F. *J. Phys. Chem. A* **1998**, *102*, 5128.

(24) Gonzalez, C.; Schlegel, H. B. *J. Phys. Chem.* **1990**, *94*, 5523.

(25) (a) Weisz, P. B. Pure *Appl. Chem.* **1980**, *52*, 2091. (b) Weisz, P. B. *ACS Symp. Ser.* **1999**, *738*, 305.

(26) Csicsery, S. M. *Stud. Surf. Sci. Catal.* **1995**, *94*, 1.

(27) Mezey, P. G. *Shape in Chemistry*; VCH Publishers: New York, 1993; pp 82−95.

(28) Lorensen, W. E.; Cline, H. E. *Computer Graphics* **1987**, *21*, 163.

(29) Breck, D. W. *Zeolite Molecular Sieves*; John Wiley & Sons: New York, 1974; pp 634−641.

(30) Scales, L. E. *Introduction to Non-Linear Optimization*; Macmillan Publishers: London, 1985.

(31) Barrer, R. M. *Zeolite and Clay Minerals as Sorbents and Molecular Sieves*; Academic Press: London, 1978; pp 65−71.

(32) Tasi et al. Under preparation.

(33) Reiss, H. *Methods of Thermodynamics*; Dover Publications: New York, 1976; pp 93−98.

(34) (a) Fukui, K.; Yonezawa, T.; Shingu, H. *J. Chem. Phys.* **1952**, *20*, 722. (b) Fukui, K.; Yonezawa, T.; Nagata, C.; Shingu, H. *J. Chem. Phys.* **1954**, *22*, 1433.

(35) (a) Politzer, P., Truhlar, D. G., Eds. *Chemical Applications of Atomic and Molecular Electrostatic Potentials*; Plenum Press: New York, 1981. (b) Tasi, G.; Pálinkó, I. *Top. Curr. Chem.* **1995**, *174*, 45 and references therein.

(36) Kiricsi, I.; Förster, H.; Tasi, G.; B. Nagy, J. *Chem. Rev.* **1999**, *99*, 2085 and references therein.

(37) Hajós, G.; Tasi, G.; Csontos, J.; Gyorffy, W.; Riedl, Zs.; Timári, G.; Messmer, A. *J. Mol. Struct.* (*THEOCHEM*) **1998**, *455*, 191.